

Growth Factor Immobilization to Synthetic Hydrogels: Bioactive bFGF-Functionalized Polyisocyanide Hydrogels

Melissa J. J. van Velthoven, Aksel N. Gudde, Evert Arendsen, Jan-Paul Roovers, Zeliha Guler, Egbert Oosterwijk, and Paul H. J. Kouwer*

With its involvement in cell proliferation, migration and differentiation basic fibroblast growth factor (bFGF) has great potential for tissue engineering purposes. So far, however, clinical translation of soluble bFGF-based therapies is unsuccessful, because the required effective doses are often supraphysiological, which may cause adverse effects. An effective solution is growth factor immobilization, whereby bFGF retains its bioactivity at increased efficacy. Studied carriers include films, solid scaffolds, and particles, as well as natural and synthetic hydrogels. However, these synthetic hydrogels poorly resemble the characteristics of the native extracellular matrix (ECM). In this work, bFGF is covalently conjugated to the synthetic, but highly biocompatible, polyisocyanide-based hydrogel (PIC-bFGF), which closely mimics the architecture and mechanical properties of the ECM. The growth factor conjugation protocol is straightforward and readily extrapolated to other growth factors or proteins. The PIC-bFGF hydrogel shows a prolonged bioactivity up to 4 weeks although no clear effects on the ECM metabolism are observed. Beyond the future potential of the PIC-bFGF hydrogel toward various tissue engineering applications, this work underlines that simple biological conjugation procedures are a powerful strategy to induce additional bioactivity in 3D synthetic cell culture matrices.

While soluble growth factor-based therapies have shown promising results in vitro,^[1] the translation to the clinical setting has not yet been successful. Soluble growth factors often suffer from a short half-life, low stability, rapid internalization by cells, and quick diffusion from the delivery site.^[2] Consequently, supraphysiological doses or multiple administrations are sometimes required to attain an effective growth factor concentration in vivo, resulting in potential adverse effects and poor cost-effectiveness of these growth factor-based therapies.^[3]

In the human body, growth factors dynamically interact with the extracellular matrix (ECM), for example, basic fibroblast growth factor (bFGF) can bind to heparan sulfate^[4] and transforming growth factor- β binds to decorin and betaglycan.^[5] In a more synthetic approach, growth factor immobilization would mimic the physiological ECM-bound presentation of growth factors.^[6] Growth factors that are covalently immobilized to hydrogels, are able to retain their effects on proliferation^[7] and ECM production.^[8] The advantages of growth factor immobilization are higher efficacy and improved functioning compared to soluble administration at similar


1. Introduction

Growth factors play a critical role in tissue repair and regeneration, and are widely investigated for tissue engineering purposes.

M. J. J. van Velthoven, E. Arendsen, P. H. J. Kouwer
Institute for Molecules and Materials
Radboud University
Heyendaalseweg 135, Nijmegen 6525 AJ, The Netherlands
E-mail: p.kouwer@science.ru.nl

M. J. J. van Velthoven, E. Arendsen, E. Oosterwijk
Department of Urology
Radboud Institute for Molecular Life Sciences
Radboud University Medical Center
Geert Grooteplein Zuid 28, Nijmegen 6525 GA, The Netherlands

A. N. Gudde, J.-P. Roovers, Z. Guler
Department of Obstetrics and Gynecology
Amsterdam University Medical Center
location AMC, Meibergdreef 9, Amsterdam 1105 AZ, The Netherlands
A. N. Gudde, J.-P. Roovers, Z. Guler
Amsterdam Reproduction and Development
Amsterdam University Medical Center
location AMC, Meibergdreef 9, Amsterdam 1105 AZ, The Netherlands

 The ORCID identification number(s) for the author(s) of this article can be found under <https://doi.org/10.1002/adhm.202301109>

© 2023 The Authors. Advanced Healthcare Materials published by Wiley-VCH GmbH. This is an open access article under the terms of the Creative Commons Attribution-NonCommercial License, which permits use, distribution and reproduction in any medium, provided the original work is properly cited and is not used for commercial purposes.

DOI: 10.1002/adhm.202301109

concentrations.^[9] Moreover, immobilization of growth factors can be spatially and, in case of non-covalent immobilization, temporally controlled.

bFGF is a frequently used growth factor for tissue engineering purposes, as it is involved in cell proliferation,^[10] migration,^[11] and differentiation.^[12] The effect of bFGF on the ECM metabolism in vitro is highly ambiguous: studies have reported contradicting stimulatory,^[13] similar^[14] and suppressive^[15] effects of bFGF on collagen production. bFGF downregulates elastin on both gene and protein level in vitro,^[16] and promotes vascular endothelial growth factor expression, which induces angiogenesis in vitro^[17] and in vivo.^[18] In vivo, bFGF has been reported to promote tissue repair of skin,^[19] bone,^[20] tendon,^[21] and cartilage.^[22] Studies on skin wound healing showed that bFGF promotes accelerated epithelization,^[19a] wound closure,^[19b] vascularization,^[19a,b] and improved regeneration of the dermis.^[19c] Analogous to in vitro findings, the effect of bFGF on collagen production in vivo is contradictory. For example, during wound healing bFGF promotes collagen production^[19a] and maturation,^[19b] whereas bFGF also can reduce scar tissue formation by suppressing collagen type I production.^[23]

Research that exploits immobilization of bFGF is focused on carriers based on films,^[24] scaffolds,^[25] particles,^[26] and hydrogels. For the latter, bFGF is mainly encapsulated in natural hydrogels^[27] or covalently immobilized to synthetic hydrogels, with the limitation that these synthetic hydrogels poorly recapitulate important features, like architecture and mechanical properties, of the native ECM.^[28]

Here, we present an approach for covalent bFGF immobilization to synthetic polyisocyanide (PIC)-based hydrogels. PIC hydrogels are highly tunable, biomimetic, and uniquely mimic the fibrous architecture and mechanical properties of the natural ECM, including strain-stiffening in the biological relevant stress regime similar to, for example, collagen.^[29] Furthermore, the thermosensitive behavior (reversible gelation upon heating at $T_{gel} \approx 15$ °C) of this hydrogel facilitates easy cell retrieval in vitro^[30] and supports minimally invasive application in vivo.^[31] PIC hydrogels can be functionalized with various bioactive molecules via a straightforward click chemistry approach.^[32] Biologically, PIC hydrogels have shown to direct stem cell fate,^[29a] facilitate vascularization^[33] and vaginal connective tissue repair in vitro,^[30b] as well as wound healing in vivo,^[31b] emphasizing the great potential of PIC hydrogels for tissue engineering purposes.

Our aim is to assess the potential of the bFGF-decorated PIC hydrogel to promote tissue regeneration in vitro. First, we covalently immobilized bFGF to PIC polymer to yield PIC-bFGF. Then we validated whether the immobilized growth factor remains bioactive in the hydrogel. Next, we investigated the effects of PIC-bFGF on cell proliferation and the ECM metabolism of adipose-derived stem cells (ASCs), whereby the latter was quantified on both gene and protein levels. The simplicity of the growth factor immobilization approach makes it similarly suited for other growth factors or bioactive molecules, which makes PIC hydrogels widely applicable for many custom biological processes, including tissue regeneration of various soft tissues.

2. Results

2.1. Preparation and Characterization of the PIC-bFGF Hydrogel

For the preparation of PIC-bFGF, we first prepared azide-appended PIC (**Figure 1A**), yielding a polymer with 3.3 mol% azide groups and a viscosity average molecular weight of 157–309 kg mol⁻¹ (for three independent batches). As the cell adhesion peptide Gly-Arg-Gly-Asp-Ser (RGD) is essential for cell-PIC matrix interactions and cell signaling, part of the azide groups (1 mol%) was used to introduce the RGD peptide through the highly efficient click chemistry approach.^[30a,34] The mechanical properties of the RGD-modified (PIC-RGD) hydrogel in PBS were analyzed with rheology (**Figure 1B,C** and **Figure S1**, Supporting Information). The properties in the linear viscoelastic regime ($G' = 95$ – 156 Pa, three batches) and the nonlinear (strain-stiffening) regime are in line with earlier work.^[30a]

To conjugate the growth factor, bFGF was equipped with dibenzocyclooctyne (DBCO) units via a flexible spacer, through *N*-hydroxysuccinimide (NHS) chemistry targeting the lysine residues (**Figure 1A**).^[35] For quantification purposes, Alexa Fluor 647 was attached to bFGF using the same NHS reaction. Analysis showed an average degree of labeling of DBCO and the fluorescent dye of 1.1 and 0.5, respectively, per bFGF molecule. Then, the DBCO-decorated growth factor was reacted with PIC-RGD in aqueous solution (4 °C) overnight (**Figure 1A**). Because of the low bFGF concentration and the high excess of reactive azide groups, we expect a high conversion of DBCO groups over the course of the reaction, which was quantified by ELISA and fluorescence measurements. For the target concentration ($[bFGF] = 2$ ng mL⁻¹), we experimentally find $[bFGF] = 2.6 \pm 0.1$ ng mL⁻¹ and a conversion of $85 \pm 2\%$. We note that in our polymers the bFGF concentration is much lower than the typical RGD concentration. In a 2 mg mL⁻¹ PIC-bFGF hydrogel, $[RGD] = 55$ μ M and $[bFGF] < 12$ nM, which amounts to less than 1 bFGF molecule per 1000 polymers. In the manuscript, most work is carried out with 50 (PIC-bFGF₅₀) or 100 ng mL⁻¹ bFGF (PIC-bFGF₁₀₀) conjugated to the polymer. Details are given in Table S1, Supporting Information.

2.2. The bFGF-Functionalized PIC Hydrogel Is Bioactive

To validate whether the bFGF bioactivity is not affected by covalent DBCO functionalization and subsequent immobilization, dose-response curves of the PIC-bFGF hydrogel and precursors were generated. Growth factor bioactivity was assessed using two different cell types: 3T3 fibroblasts and primary ASCs. The latter is our cell type of interest as they are often used for tissue engineering applications.^[36] As the default cell line to determine the bioactivity of growth factors, 3T3 fibroblasts were used to validate the activity of PIC-bFGF with soluble bFGF and bFGF-DBCO controls, tested both in a 2D and 3D setting. Following the thorough validation in 3T3 fibroblasts, we determined the bioactivity of PIC-bFGF in ASCs. bFGF-DBCO treatment on 2D cultured 3T3 fibroblasts induced a threefold increase in proliferation (**Figure 2A**), similar to the increase in proliferation of the control (3T3 fibroblasts treated with soluble bFGF, **Figure S2A**, Supporting Information). The results show that the introduction

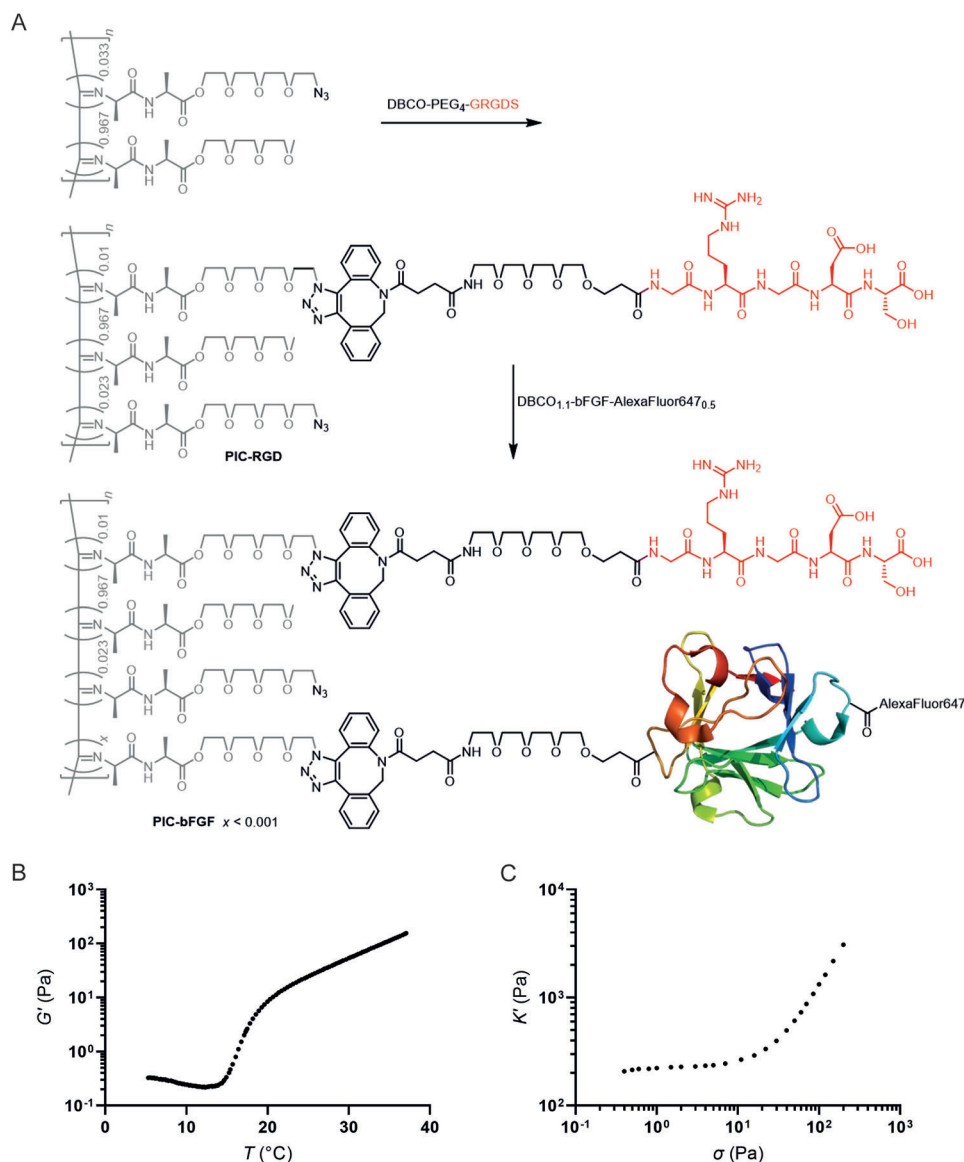


Figure 1. Molecular structure and mechanical properties of PIC-based hydrogels. A) Preparation and molecular structure of PIC-RGD and PIC-bFGF. Mechanical properties of the PIC-RGD hydrogel: B) The storage modulus (G') shows temperature-induced gelation at approximately 20 °C; C) the differential modulus (K') shows strain-induced stiffening. Loss data is given in Figure S1, Supporting Information.

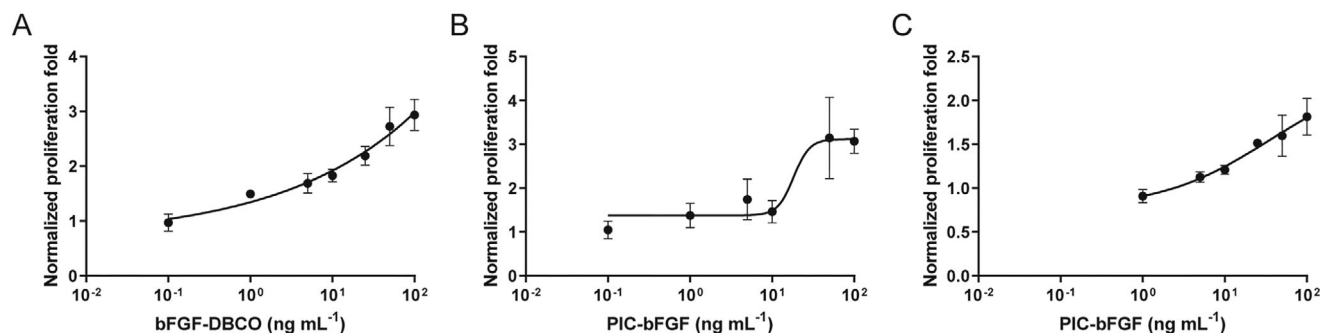


Figure 2. The PIC-bFGF hydrogel is bioactive. Dose-response curves of bFGF-DBCO treatment on A) 2D cultured 3T3 fibroblasts, B) 3T3 fibroblasts encapsulated in the PIC-bFGF hydrogel ($EC_{50} = 18.3 \text{ ng mL}^{-1}$), and C) ASCs encapsulated in the PIC-bFGF hydrogel ($EC_{50} = 36.1 \text{ ng mL}^{-1}$). Lines are fit to a four-parameter dose-response function ($n = 3$).

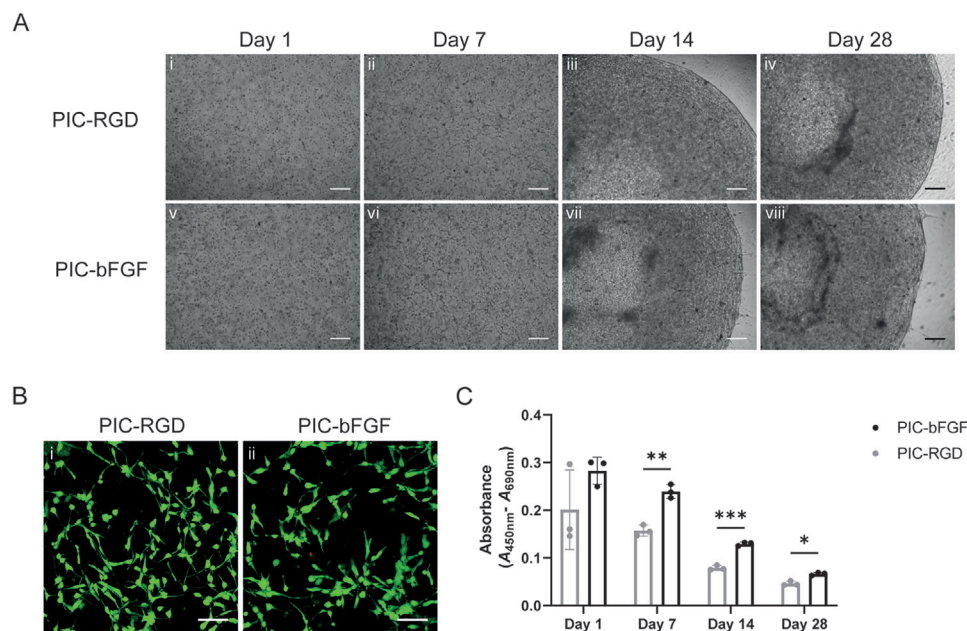


Figure 3. PIC-bFGF hydrogels remain bioactive for 28 days. A) Representative brightfield images of ASCs encapsulated in the PIC-RGD and PIC-bFGF₁₀₀ hydrogels up to 28 days in culture. B) ASCs encapsulated in PIC-RGD and PIC-bFGF₅₀ hydrogels are viable at day 7 (live = green and dead = red). C) PIC-bFGF₁₀₀ promotes the proliferation of ASCs compared to PIC-RGD at day 7 ($p = 0.007$), 14 ($p = 0.001$), and 28 days ($p = 0.023$). Statistical analysis with a two-way ANOVA followed by Šídák's multiple comparisons test ($n = 3$). Scale bar = A) 250 and B) 100 μm .

of linking groups on bFGF does not compromise its bioactivity. In a 3D setting, soluble bFGF treatment on 3T3 fibroblasts encapsulated in the PIC-RGD hydrogel also resulted in a similar proliferation increase as the 2D cultured 3T3 fibroblasts (Figure S2B, Supporting Information). Likewise, the 3T3 fibroblast cultured in the PIC-bFGF hydrogel showed a similar threefold increase in proliferation albeit with an increased half-maximal effective concentration (EC_{50}) compared to the soluble control (Figure 2B). Last, we confirmed that the PIC-bFGF hydrogel is bioactive when cultured with ASCs, albeit with a reduced fold in proliferation compared to 3T3 fibroblasts (Figure 2C).

2.3. bFGF-Functionalized PIC Hydrogels Remain Bioactive for 28 Days

To assess whether the PIC-bFGF hydrogel remains bioactive for a sustained period in long-term cultures, ASCs were cultured for up to 28 days in PIC-bFGF or, as a control, in PIC-RGD. At day 1, the ASCs exhibit a round morphology in both matrices (Figure 3Ai,v). After 7 days, elongated cell morphologies (Figure 3Aii,vi) were observed. Two weeks' post-encapsulation, both the PIC-RGD and PIC-bFGF hydrogels started to contract as a result of the contractile forces that the ASCs apply on their microenvironment (Figure 3Aiii,iv,vii,viii). Cell viability analysis showed viable cells in both the PIC-RGD and PIC-bFGF hydrogels (Figure 3B). ASCs cultured in the PIC-bFGF hydrogel showed a significant increase in proliferation 7, 14, and 28 days' post-encapsulation (Figure 3C), which confirms the continued bioactivity of the PIC-bFGF hydrogel. We note that the decrease in proliferation over time results from the fact that the cells

were cultured under starved conditions in order to measure the bioactivity of PIC-bFGF.

2.4. Immobilization of bFGF Has No Effect on Collagen and Elastin Deposition on ASCs Encapsulated in PIC Hydrogels

Effects of the PIC-bFGF hydrogel on ECM metabolism were assessed by quantifying collagen and elastin production on protein level as well as quantifying collagen production based on imaging. At day 1, ASCs encapsulated in PIC-RGD and PIC-bFGF hydrogels predominantly show collagen as dotted structures (Figure 4Ai–iv), which is indicative of intracellular procollagen assembly.^[37] After 7 days, next to dotted structures, fiber-like structures are visible in both PIC-RGD and PIC-bFGF (Figure 4Av–viii), which indicates extracellular collagen fiber formation.^[37] At 14 and 28 days' post-encapsulation, all hydrogels show more deposited (mature) collagen fibers compared to day 7 as well as contraction of the 3D cultures (Figure 4Aix–xvi). Collagen quantification based on fluorescence intensity at day 14 showed no difference between the PIC-RGD and PIC-bFGF hydrogels (Figure 4B), whereby we emphasize that the collagen fluorescence intensities were normalized to the nuclear fluorescence intensity (cell density) to exclude the effects of contraction and differences in proliferation.

Collagen quantification on protein level, using a picosirius red-based assay, shows no significant differences between PIC-RGD and PIC-bFGF at all four time points (Figure 4C), which is consistent with the fluorescence intensity data. We do observe a significant increase in collagen production over time (Figure S3, Supporting Information), whereby the amount of collagen doubled at days 7 and 28 compared to day 1 in both hydrogels. When

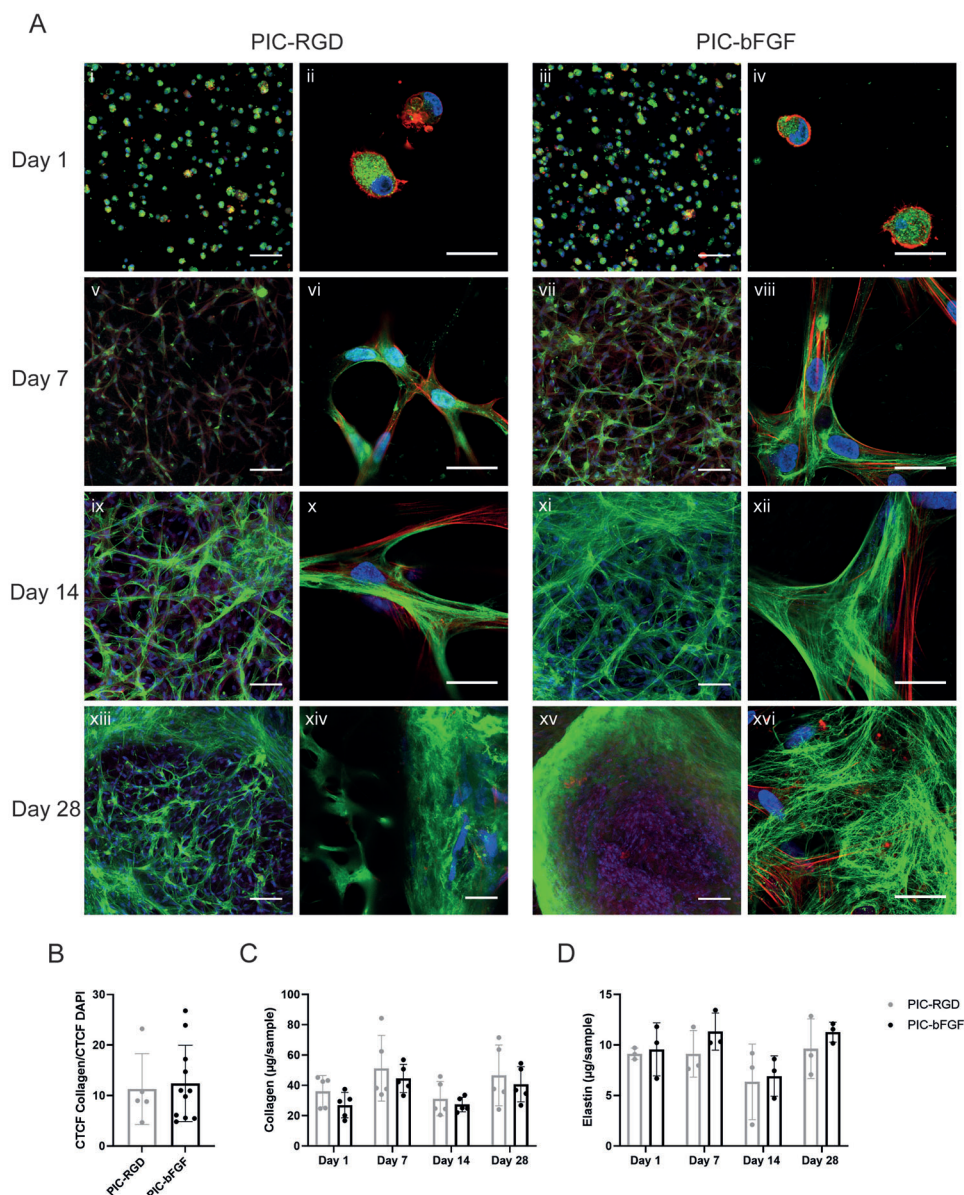


Figure 4. The PIC-bFGF hydrogel does not promote collagen and elastin deposition of ASCs. A) Representative confocal images of deposited collagen by ASCs encapsulated in the PIC-RGD and PIC-bFGF₅₀ hydrogels at days 1–28 (collagen = green, F-actin = red and nuclei = blue; scale bar = 100 (first and third column) and 25 μm (second and fourth column)). B) Corrected total cell fluorescence (CTCF) analysis of collagen (normalized to the CTCF of DAPI) at day 14 ($n \geq 5$; unpaired t -test). Protein quantification shows similar results between ASCs encapsulated in PIC-RGD and PIC-bFGF₁₀₀ for both C) collagen ($n = 5$) and D) elastin ($n = 3$) at all time points. Statistical analyses were conducted with two-way ANOVA followed by a (C) Šidák's multiple comparisons test or (D) Tukey's and Šidák's multiple comparisons test.

we studied the correlation between the conjugated bFGF concentration and collagen production, we only observed an increase in collagen production in PIC-bFGF₅₀ compared to PIC-bFGF₁₀ ($p = 0.034$) and PIC-bFGF₁₀₀ ($p = 0.036$) at day 7 (Figure S3, Supporting Information). We note that the amount of collagen produced in the PIC-bFGF₅₀ hydrogel was equal to the PIC-RGD hydrogel.

Analogous to collagen, elastin production is similar between the ASCs cultured in PIC-RGD and PIC-bFGF hydrogels over time (Figure 4D). Overall, we conclude that immobilization of

bFGF to the PIC-RGD hydrogel has no effect on collagen and elastin production.

2.5. The Effect of PIC-bFGF on the Expression of ECM-Related Genes

In addition to our studies at protein level, we quantified bFGF-induced changes at gene expression level. Expression of *COL1A1*, *COL3A1*, and *ELN* are related to ECM production,

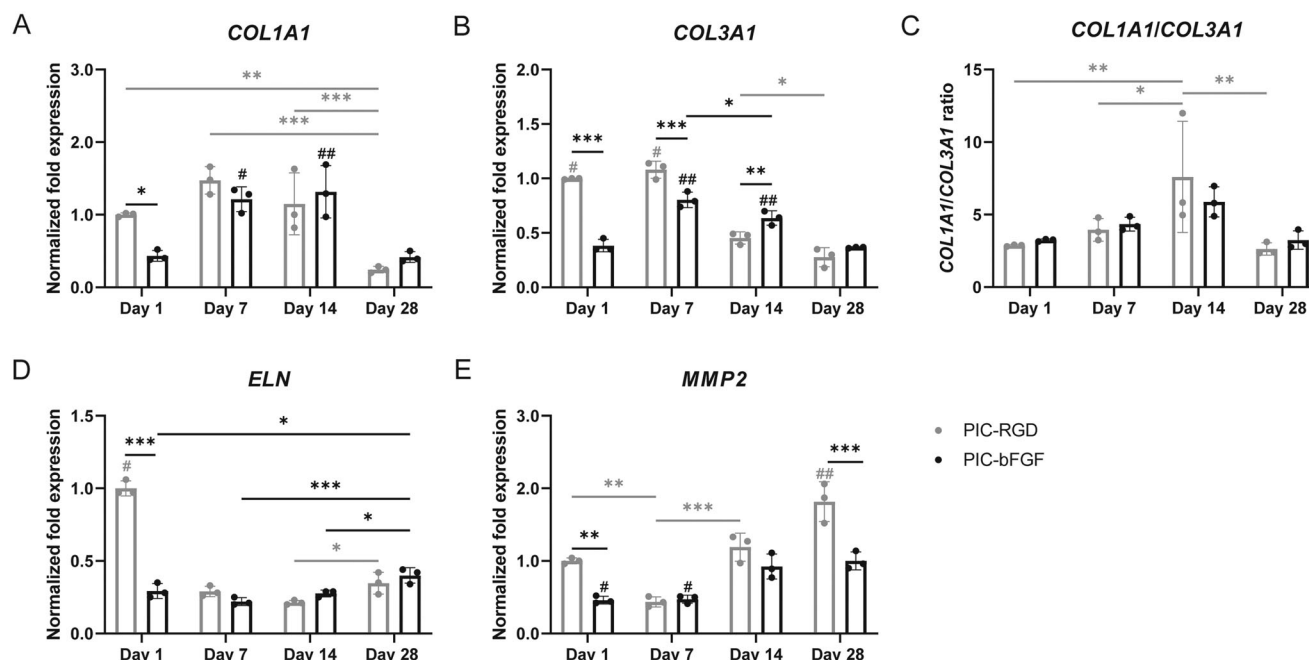


Figure 5. The effect of the PIC-bFGF hydrogel on the expression of ECM-related genes. Gene expression levels from days 1–28 of ASCs cultured in PIC-RGD and PIC-bFGF₁₀₀ hydrogels for A) *COL1A1*, B) *COL3A1*, C) *COL1A1/COL3A1* ratio, D) *ELN*, and E) *MMP2*. Statistical analyses were performed using two-way ANOVAs with Tukey's and Šidák's multiple comparisons test ($n = 3$; * $p < 0.05$, ** $p < 0.01$, *** $p < 0.001$). A) # marks that *COL1A1* is higher expressed in PIC-bFGF at day 7 compared to days 1 and 28 ($p \leq 0.003$). ## marks an increased *COL1A1* expression in PIC-bFGF at day 14 compared to days 1 and 28 ($p < 0.001$). B) # illustrates that *COL3A1* is higher expressed in PIC-RGD at days 1–7 compared to days 14–28 ($p < 0.001$) and ## marks that in PIC-bFGF the expression increased at days 7 and 14 compared to days 1 and 28 ($p < 0.001$). D) # marks that *ELN* expression in PIC-RGD is higher at day 1 compared to days 7–28 ($p < 0.001$). E) # illustrates that *MMP2* is lower expressed at days 1–7 compared to days 14–28 in PIC-bFGF ($p \leq 0.008$); and ## marks an increased expression in PIC-RGD at day 28 compared to days 1–14 ($p < 0.001$).

whereas *MMP2* expression is associated with ECM degradation. ASCs encapsulated in the PIC-bFGF hydrogel show a downregulation of *COL1A1* ($p = 0.025$), *COL3A1* ($p < 0.001$), *ELN* ($p < 0.001$), and *MMP2* ($p = 0.001$) at day 1 compared to PIC-RGD (Figure 5). *COL3A1* is downregulated at day 7 ($p < 0.001$) and upregulated at day 14 ($p = 0.008$) in PIC-bFGF (Figure 5B). *MMP2* expression is reduced at day 28 ($p < 0.001$) in the PIC-bFGF hydrogel (Figure 5E). Pooling the results of two separate experiments together reduces the differences in gene expression between PIC-RGD and PIC-bFGF at day 7 (Figure S4, Supporting Information).

Furthermore, we analyzed whether gene expression alters over time. In the PIC-RGD hydrogels, *ELN*, *COL3A1*, and *COL1A1* are significantly downregulated from days 7, 14, and 28 onward respectively (Figure 5A,B,D), whereas *MMP2* is significantly upregulated at day 28 (Figure 5E). Furthermore, the *COL1A1/COL3A1* ratio is significantly higher at day 14 (Figure 5C). This ratio is particularly relevant as an ECM remodeling indicator in a clinical context.^[38]

In the PIC-bFGF hydrogels, *COL1A1* and *COL3A1* are significantly upregulated at days 7 and 14 (Figure 5A,B) and *MMP2* at days 14 and 28 (Figure 5E). The expression of *ELN* remains unchanged over time, with a minor increase at day 28 (Figure 5D). Overall, except for downregulation at day 1, the expression levels of ECM-related genes remain similar between PIC-RGD and PIC-bFGF hydrogels, but their expression alters over time.

3. Discussion

In this study, we present a bFGF-functionalized PIC hydrogel. The PIC hydrogel is known to mimic the architecture and mechanical properties of the native ECM, and this manuscript investigated how decoration with bFGF increased its potential to promote tissue regeneration in vitro. Our data showed that the PIC-bFGF hydrogel is bioactive and remains bioactive for a month. However, we do not observe strong effects of bFGF immobilization on the PIC hydrogel on the ECM metabolism of ASCs.

3.1. PIC-bFGF Preparation

Covalent immobilization of bFGF to PIC-RGD using click chemistry has the following advantages: prevention of a bulk release and prolonged bioactivity without the use of multiple administrations of bFGF.^[39] The DBCO-based click chemistry procedure allows excellent control over the degree of labeling and the concentration of the immobilized growth factor in the hydrogel. The conjugation procedure is directly translatable toward other growth factors and other active biomolecules, which has been demonstrated earlier for comparable polymer systems.^[40]

3.2. PIC-bFGF Bioactivity

We thoroughly validated the bioactivity of the PIC-bFGF hydrogel, because one could have expected that bFGF immobiliza-

tion negatively impacts the binding affinity of bFGF to the fibroblast growth factor receptor (FGFR).^[1] 3T3 fibroblasts, which is a common cell line for bioactivity assessments, responded to PIC-bFGF with increased proliferation in a dose-dependent manner. To compare the bioactivity to traditional 2D cell culture assessment,^[24] we included a 2D control in which bFGF exhibited an EC_{50} similar to the value reported by the manufacturer. The introduction of the DBCO-handle, necessary for subsequent conjugation, did not reduce the bioactivity of bFGF. 3T3 fibroblasts in a 3D PIC-bFGF microenvironment yielded a similar proliferation increase as the soluble bFGF, indicating full bioactivity of bFGF conjugated to the PIC polymer. Earlier work also demonstrated that the activity of large biomolecules is not necessarily compromised by covalent conjugation to the PIC polymers.^[40]

The bioactivity of immobilized bFGF is strongly dose-dependent, which emphasizes the importance to measure dose-response curves. Other studies that compared the bioactivity of bFGF-immobilized biomaterials (against the same material without bFGF) did not provide dose-response curves^[24,25a,25b,26a,26b,41] or, when they did, they did not determine the corresponding EC_{50} .^[26c] Other studies investigated the potential effect of immobilization on bioactivity using additional controls such as soluble bFGF.^[25c,42] Overall, there is a clear lack of detailed bioactivity data of bFGF-immobilized biomaterials in the literature, which makes it difficult to compare the effects of immobilization between different studies.

ASCs are known to contribute to tissue regeneration,^[36] which motivated us to use ASCs to evaluate the potential of PIC-bFGF for tissue engineering purposes. Compared to the 3T3 fibroblasts, the response of ASCs toward PIC-bFGF is less pronounced, which may be the consequence of the less proliferative character of the primary ASCs. Moreover, one would expect the EC_{50} to vary per cell type,^[43] which we also found experimentally; the EC_{50} for the ASCs is higher than for the 3T3 fibroblasts. Overall, the results confirm that the conjugation of bFGF to the PIC polymer does not affect the bioactivity.

In contrast to other studies that only reported bioactivity data after several days in culture,^[24] we showed that PIC-bFGF exhibits a long-term bioactivity for a month as a result of the covalent immobilization that prevents an undesired bulk release from the hydrogel.^[44] One needs to take into account that a potential disadvantage of this strategy is that crowding can impede the binding interactions of bFGF with the FGFR.^[45] Future work can, for instance, focus on incorporating protease-sensitive linkers in order to achieve a controlled release of bFGF from the PIC hydrogel.^[46]

3.3. Impact on the ECM

PIC decoration with bFGF has no substantial effect on collagen deposition, which corresponds with the current literature that reports ambiguous results.^[13–15] The unaffected collagen deposition is confirmed on gene level: *COL1A1* is downregulated in PIC-bFGF at day 1 and is similarly expressed between the PIC-bFGF and PIC-RGD hydrogel at the other time points. These results are in line with earlier studies that report that bFGF downregulates *COL1A1* expression in lung fibroblasts,^[47] hepatic stellate cells,^[48] osteoblast-like cells,^[49] periodontal ligament cells^[50]

and valvular interstitial cells.^[51] It is important to note that for ASCs, *COL1A1* is already highly expressed in the absence of bFGF ($C_q \approx 14$), and direct effects from bFGF are negligible.

Analogous to the collagen, the conjugated growth factor has no effect on elastin deposition on protein level. Gene expression of *ELN* in the PIC-bFGF hydrogel is downregulated on day 1, which is in line with other studies.^[16,52] For example, it has been reported that bFGF downregulates *ELN* in smooth muscle cells^[16] and fibroblasts.^[52] A suggested cause of *ELN* downregulation by bFGF signaling is the induction of Fra-1 that forms a heterodimer with c-Jun, resulting in an inhibitory complex that can bind to the elastin promoter.^[52] *MMP2* is downregulated in PIC-bFGF on days 1 and 28 compared to PIC-RGD; other studies reported a slight upregulation of *MMP2* upon bFGF treatment both in vitro^[51] and in vivo.^[53]

4. Conclusion

Previous studies clearly indicated that bFGF has an active role in tissue regeneration in vivo.^[19,20,22] Based on the analogous in vitro results of PIC-bFGF with soluble bFGF found in this work, it would make sense to investigate PIC-bFGF for tissue regeneration in vivo. After bFGF concentrations on the polymer have been optimized per application, in vivo studies for skin,^[19a] ligament and tendon,^[54] cartilage,^[22a] pelvic floor^[55] and vasculature^[56] are foreseeable. This work demonstrates the advantages of covalent conjugation: excellent dosage control and prolonged bioactivity. Precisely regulating bioactivity in this way may contribute to preventing excessive ECM production in vivo, which is a crucial step in the development of anti-fibrotic biomaterials. Moreover, using the straightforward click chemistry approach, the PIC hydrogel can be equipped with a myriad of bioactive molecules including other growth factors, which creates a versatile toolbox of customized biomaterials for (soft) tissue engineering applications.

5. Experimental Section

Synthesis of the PIC-RGD Hydrogel: The PIC polymers were synthesized as previously described.^[57] In brief, tri(ethylene glycol) substituted isocyanato-(D)-alanyl-(L)-alanine monomers and corresponding azide-appended monomers were copolymerized at a 30:1 ratio using $Ni(ClO_4)_2 \cdot 6 H_2O$ as catalyst (catalyst to total monomer ratio = 1:2000). The PIC polymers were functionalized with RGD motifs as previously described.^[30a] First, the GRGDS peptide (H-Gly-Arg-Gly-Asp-Ser-OH, Bachem, Switzerland) was conjugated to a DBCO-PEG₄-NHS spacer (Click Chemistry Tools, USA) and full conversion of the reaction was validated with mass spectrometry. The conjugate was subsequently reacted, through strain-promoted azide-alkyne cycloaddition, with the azide-appended PIC polymer in acetonitrile (ACN) to yield the PIC-RGD polymer. Full conversion yields a concentration of 55 μM RGD at a polymer concentration of 2 mg mL⁻¹. The PIC-RGD polymer was sterilized with UV for 10 min and subsequently dissolved in sterile PBS at a concentration of 4 mg mL⁻¹ on a rotor at 4 °C for approximately 2 days. The PIC-RGD solutions were aliquoted and stored at -20 °C until further use. Viscosity average molecular weights (M_v) of the PIC polymers were determined from the intrinsic viscosities, following previously described methods.^[57a]

Rheological measurements of the PIC-RGD hydrogels (2 mg mL⁻¹ in PBS) were performed on a rheometer (Discovery HR-2, TA Instruments, USA) using a steel parallel plate geometry (diameter = 40 mm, gap = 500 μm). The samples were subjected to a temperature ramp from $T = 5-7$ °C (1 °C min⁻¹, strain $\gamma = 1\%$ and frequency $\omega = 1$ Hz) to determine

the storage (G') and loss (G'') moduli. The nonlinear mechanics were determined from a prestress protocol, whereby an increased prestress (0.4–200 Pa) was applied to the sample. The differential modulus (K') was calculated from small superposed oscillatory stress and the corresponding strain values at $\omega = 1$ Hz.

For this study, three similar PIC-RGD hydrogel batches have been used with the following properties: $G' = 95$ Pa ($M_v = 295$ kg mol $^{-1}$), $G' = 111$ Pa ($M_v = 157$ kg mol $^{-1}$) and $G' = 156$ Pa ($M_v = 309$ kg mol $^{-1}$).

Preparation of the PIC-bFGF Hydrogels: To functionalize the PIC-RGD hydrogel with bFGF, the bFGF was coupled to a DBCO-terminated spacer analogous to a literature procedure.^[35] Recombinant human bFGF (Peprotech, USA) was dissolved in 1 mg mL $^{-1}$ PBS and transferred to a 10 kDa cutoff spin filter (Amicon Ultra, Merck, Germany) and centrifuged three times at 4000 rpm for 7 min at 4 °C to remove any residual Tris buffer. Subsequently, the bFGF concentration was determined at 280 nm using the molar extinction coefficient of 16 180 m $^{-1}$ cm $^{-1}$ with a NanoDrop ND-1000 spectrophotometer (Thermo Fisher Scientific, USA). To the washed bFGF, 3 equivalents of DBCO-PEG $_4$ -NHS (100 mM DMSO, Click Chemistry Tools, USA) and 1.5 equivalent of Alexa Fluor 647 NHS ester (10 mM in DMSO, Thermo Fisher Scientific, USA) were added and the solution ($c_{bFGF} = 0.704$ mg mL $^{-1}$ and $v_{reaction} = 957$ μ L) was gently shaken. The mixture was incubated on a rotor at 7 rpm for 3 h at 4 °C. Subsequently, bFGF-DBCO was purified and concentrated by centrifuging five times at 4000 rpm for 7 min at 4 °C using a 10 kDa cutoff spin filter. The concentration of purified bFGF-DBCO and the degree of labeling (DBCO-PEG $_4$ -NHS and Alexa Fluor 647 NHS) were determined using the NanoDrop ND-1000 spectrophotometer from the absorbances at 280, 309, and 649 nm, respectively. Finally, 1% w/v BSA/PBS (Sigma Aldrich, USA) was added to the bFGF-DBCO resulting in the final bFGF-DBCO product dissolved in 0.1% BSA/PBS, which was aliquoted and stored at -80 °C.

The bFGF-DBCO was conjugated to the dissolved PIC-RGD hydrogel (PIC-bFGF) overnight on a rotor at 4 °C to a final concentration of 200 ng mL $^{-1}$ and stored at -20 °C until further use. The conversion of bFGF-DBCO conjugated to the PIC-RGD was determined by incubating the PIC-bFGF hydrogels in PBS for 24 h, to allow the diffusion of the unbound bFGF-DBCO into the supernatant. After the incubation period, the fluorescent intensities of the supernatants and the liquified PIC-bFGF solutions were measured on the Spark 10M multimode plate reader ($\lambda_{excitation} = 635$ nm, $\lambda_{emission} = 680$ nm, Tecan, Switzerland). To validate the bFGF concentration, bFGF-DBCO and the PIC-bFGF hydrogel were analyzed in triplicate using the human FGF-basic Mini ABTS ELISA development kit (Peprotech, USA) according to manufacturer's protocol. The absorbances were measured at 5-min intervals for 45 min at 405 nm (reference = 650 nm) using the Spark 10M multimode plate reader.

In this study, PIC-bFGF hydrogels were prepared with bFGF concentrations ranging from 0.01 to 100 ng mL $^{-1}$ (PIC-bFGF $_{0.01}$ -PIC-bFGF $_{100}$). To keep the RGD concentration constant, the PIC-bFGF hydrogel was diluted with the PIC-RGD hydrogel. Detailed hydrogel conditions per experiment are summarized in Table S1, Supporting Information.

Cell Culture: Informed written consent was obtained prior to the research. Human adipose tissue samples of two patients were obtained at the Department of Plastic Surgery (RaboudUMC, Nijmegen, the Netherlands). The ASCs were isolated as previously described^[58] and used for experiments at passage 5. ASCs were cultured in minimum essential medium alpha (MEM α ; Gibco, Thermo Fisher Scientific, USA) supplemented with 10% fetal calf serum (FCS; Sigma Aldrich, USA) and 1% penicillin/streptomycin (100 U mL $^{-1}$ and 100 μ g mL $^{-1}$, Gibco, Thermo Fisher Scientific, USA). 3T3 fibroblasts were purchased from ATCC and cultured in Dulbecco's modified Eagle's medium (DMEM; Gibco, Thermo Fisher Scientific, USA) supplemented with 1% glutamine (2 mM, Life Technologies, Thermo Fisher Scientific, USA) and 10% FCS. In the case of basal medium, unsupplemented DMEM was used and MEM α was solely supplemented with 1% penicillin/streptomycin.

Cell Encapsulation: In general, cells were encapsulated in the PIC-RGD and PIC-bFGF hydrogels by mixing equal volumes of cell solution (either ASCs or 3T3 fibroblasts) and polymer solution on ice and pipetted in 96-well plates (100 μ L) or microplates (10 μ L, Ibidi, Germany), resulting in a final polymer concentration of 2 mg mL $^{-1}$ and a cell density of 10 6 cells

mL $^{-1}$ (ASCs) or 250 000 cells mL $^{-1}$ (3T3 fibroblasts). To induce gelation, the plates were immediately incubated for >5 min at 37 °C. Subsequently, the corresponding medium was added to the hydrogels (100 μ L for 96-well plates and 50 μ L for microplates) and incubated at 37 °C and 5% CO $_2$, the medium was refreshed three times per week. Brightfield microscopy images were taken using an inverted microscope (Leica DMI1). Detailed culture conditions per experiment are summarized in Table S1, Supporting Information.

Cell Culture for the Bioactivity Experiments: For the 2D bioactivity experiments, 3T3 fibroblasts were seeded in full DMEM (1750 cells/well in a 96-well plate). The next day, the full medium was removed, and the culture was washed with PBS and changed to basal DMEM to starve the cells for 24 h. After starvation, the cells were treated for 3 days with basal DMEM supplemented with bFGF-DBCO (0.1–100 ng mL $^{-1}$ in 0.1% BSA/PBS) or bFGF (0.01–10 ng mL $^{-1}$ in 0.1% BSA/PBS). For the 3D bioactivity experiments, 3T3 fibroblasts were starved in basal DMEM for 24 h in culture flasks, after which the fibroblasts were encapsulated in PIC-RGD and PIC-bFGF (0.1–100 ng mL $^{-1}$) hydrogels at a final concentration of 250 000 cells mL $^{-1}$. Bioactivity was assessed with CellTiter-Glo after 3 days. The ASCs were starved for 24 h in basal MEM α and subsequently encapsulated in PIC-RGD and PIC-bFGF (1–100 ng mL $^{-1}$) hydrogels at a final concentration of 500 000 cells mL $^{-1}$. Bioactivity was assessed with WST-1 after 7 days.

Cell Proliferation and Viability: 3T3 fibroblast bioactivity was assessed with CellTiter-Glo (Promega, USA) following the manufacturer's instructions. For the 3D experiments, the excess medium was removed, and the hydrogels were incubated for 20 min at 4 °C. The liquified hydrogels were resuspended with 100 μ L of CellTiter-Glo, mixed for 2 min to induce cell lysis, and incubated for 10 min at room temperature. Luminescence was recorded using the Victor 3 1420 multilabel plate counter (PerkinElmer, USA). To assess the bioactivity and proliferation of the ASCs, the samples were incubated for 1 h (37 °C and 5% CO $_2$) with RPMI 1640 (Gibco, Thermo Fisher Scientific, USA) supplemented with 10% WST-1 (Roche, Germany). The absorbances of the supernatants were measured with a Spark 10M multimode plate reader at 450 nm (reference = 690 nm).

Cell viability of the ASCs was determined with the LIVE/DEAD Viability/Cytotoxicity kit (1 h incubation of 8 μ M Calcein AM and 4 μ M Ethidium homodimer-1 in full MEM α , Invitrogen, Thermo Fisher Scientific, USA). Subsequently, the samples were washed three times for 5 min with PBS and directly imaged using a confocal laser scanning microscope (Zeiss LSM 900).

Confocal Imaging of Deposited Collagen: An Oregon Green labeled collagen binding protein probe (CNA35-OG488) was used to visualize collagen deposition in the hydrogels.^[59] In brief, the samples were fixed in 3% paraformaldehyde for 30 min at 37 °C, washed with PBS, and incubated overnight at 37 °C with 1 μ M CNA35-OG488 (Department of Biomedical Engineering, Eindhoven University of Technology, The Netherlands). Next, the samples were stained for 1 h with Texas Red X-Phalloidin (1:200; Invitrogen, Thermo Fisher Scientific, USA) and 15 min with DAPI (10 μ g mL $^{-1}$; Merck, Germany). Between incubation steps, the hydrogels were washed three times 5 min with PBS. The samples were imaged using a confocal laser scanning microscope (Zeiss LSM 900). To quantify the fluorescence intensity of collagen; the integrated density, area, and mean gray values (mean of three background regions) were measured for each image using Fiji, and the corrected total cell fluorescence was calculated (CTCF = integrated density – (area of selected cell \times mean fluorescence of background readings). The CTCF of CNA35 was normalized to the CTCF of DAPI.

Quantification of Collagen and Elastin Production: Quantification of collagen and elastin production was performed as previously described.^[30b] In brief, after medium removal and the addition of cold PBS, the hydrogels were incubated for 20 min at 4 °C to liquefy the PIC polymer solution. For collagen quantification, three wells were pooled for one sample whereas for elastin quantification one well was used per sample. The liquified PIC hydrogel solution was removed, and the samples were washed twice with PBS by centrifuging at 2500 g for 5 min at 4 °C. The samples were mechanically disrupted using a pellet pestle motor (Kimble, USA); disruption was performed after the last washing step in PBS (elastin quantification)

Table 1. Primer sequences used for qPCR.

Gene		Sequences
COL1A1	Forward	5' TCCAACGAGATCGAGATCC 3'
	Reverse	5' AAGCCGAATTCCTGGTCT 3'
COL3A1	Forward	5' GATCCGTTCTCTGCGATGAC 3'
	Reverse	5' AGTTCTGAGGACCACTAGGG 3'
ELN	Forward	5' TTTGGCCCGGAGTAGTTGG 3'
	Reverse	5' CAGCTGCTTCTGGTGACACAAC 3'
HPRT1	Forward	5' GCTGACCTGCTGGATTACAT 3'
	Reverse	5' CTGCGACCTTGACCATCT 3'
MMP2	Forward	5' TCCAAGTCTGGAGCGATGTG 3'
	Reverse	5' CCGTCTTACCGTCAAAGGG 3'
YWHAZ	Forward	5' GATGAAGCCATTGCTGAACCTG 3'
	Reverse	5' CTATTGTGGGACAGCATGGA 3'

COL1A1, collagen type I alpha 1 chain; COL3A1, collagen type III alpha 1 chain; ELN, elastin; HPRT1, hypoxanthine phosphoribosyltransferase 1; MMP2, matrix metalloproteinase 2; YWHAZ, tyrosine 3-monooxygenase/tryptophan 5-monooxygenase activation protein zeta.

or after adding 10% w/v polyethylene glycol 6000 (Merck, Germany) for collagen quantification. Elastin and collagen concentrations were quantified, using the Fastin Elastin Assay (Biocolor Ltd., UK) and a picosirius red-based assay respectively, as previously described.^[30b] The absorbance values of the collagen and elastin samples were measured at 540 and 513 nm respectively with the Spark 10M multimode plate reader. The absorbance values were converted into masses based on standard lines of rat tail-derived collagen type I (Merck, Germany) and soluble α -elastin (Biocolor Ltd., UK) respectively.

Quantitative Real-Time PCR: To isolate RNA from the samples, the medium was removed, and cold PBS was added to the hydrogels, which were incubated for 20 min at 4 °C. Subsequently, three hydrogels were collected per sample, and centrifuged at 2500 g for 5 min at 4 °C to obtain a cell pellet. A lysis buffer (RLT buffer, Qiagen, Germany), supplemented with 1% β -mercaptoethanol, was added to the cell pellets, these pellets were subsequently mechanically disrupted using a pellet pestle motor. RNA was isolated with the RNeasy Plus Mini Kit according to the manufacturer's protocol (Qiagen, Germany). RNA concentrations were measured on a NanoDrop ND-1000 spectrophotometer (Thermo Fisher Scientific, USA). The RNA was reverse transcribed using the SuperScript II Reverse Transcriptase kit (Invitrogen, Thermo Fisher Scientific, USA). Quantitative real-time PCR (qPCR) was performed using the SYBR Green I master mix (Roche, Germany) with the corresponding primers (Table 1) and measured using the LightCycler 480 (Roche, Germany). Expression levels were normalized to the geometric mean of the two house-keeping genes (HPRT1 and YWHAZ) and normalized to the fold change of the PIC-RGD hydrogel samples at day 1.

Statistical Analysis: Statistical analyses were performed using GraphPad Prism version 9.0 (GraphPad Software Inc., USA). The half-maximal effective concentrations (EC₅₀) were calculated with the built-in four-parameter dose-response function. Unpaired *t*-tests were performed to compare two groups with one variable. A two-way ANOVA with subsequent Tukey's and/or Sidak's multiple comparisons tests was conducted to analyze two or more groups with multiple variables. Differences were considered significant at $p < 0.05$ (* $p < 0.05$, ** $p < 0.01$ and *** $p < 0.001$). The data are presented as the mean \pm standard deviation.

Supporting Information

Supporting Information is available from the Wiley Online Library or from the author.

Acknowledgements

This project received public funding from ZonMw for the TOP project (grant number: 91218030). The authors acknowledge Dr. Roel Hammink for his input on the bFGF-DBCO synthesis and Dr. Behrad Shaghghi for helping with the polymer synthesis and characterization.

Conflict of Interest

The authors declare no conflict of interest.

Data Availability Statement

The data that support the findings of this study are available from the corresponding author upon reasonable request.

Keywords

basic fibroblast growth factor, bioactivity, growth factor immobilization, polyisocyanide hydrogels, tissue engineering

Received: April 8, 2023

Revised: July 22, 2023

Published online: August 10, 2023

- [1] K. Lee, E. A. Silva, D. J. Mooney, *J. R. Soc., Interface* **2011**, *8*, 153.
- [2] A. C. Mitchell, P. S. Briquez, J. A. Hubbell, J. R. Cochran, *Acta Biomater.* **2016**, *30*, 1.
- [3] X. Ren, M. Zhao, B. Lash, M. M. Martino, Z. Julier, *Front. Bioeng. Biotechnol.* **2020**, *7*, 469.
- [4] J. Schlessinger, A. N. Plotnikov, O. A. Ibrahim, A. V. Eliseenkova, B. K. Yeh, A. Yayon, R. J. Linhardt, M. Mohammadi, *Mol. Cell* **2000**, *6*, 743.
- [5] R. Drogue, C. Cabello-Verrugio, C. Riquelme, E. Brandan, *Matrix Biol.* **2006**, *25*, 332.
- [6] D. Enriquez-Ochoa, P. Robles-Ovalle, K. Mayolo-Deloya, M. E. G. Brunck, *Front. Bioeng. Biotechnol.* **2020**, *8*, 821.
- [7] T. Bavaro, S. Tengattini, R. Rezwan, E. Chiesa, C. Temporini, R. Dorati, G. Massolini, B. Conti, D. Ubiali, M. Terreni, *Sci. Rep.* **2021**, *11*, 2629.
- [8] B. K. Mann, R. H. Schmedlen, J. L. West, *Biomaterials* **2001**, *22*, 439.
- [9] A. Cipitria, M. Salmeron-Sanchez, *Adv. Healthcare Mater.* **2017**, *6*, 1700052.
- [10] T. L. Hebert, X. Wu, G. Yu, B. C. Goh, Y. D. Halvorsen, Z. Wang, C. Moro, J. M. Gimble, *J. Tissue Eng. Regen. Med.* **2009**, *3*, 553.
- [11] B. Awan, D. Turkov, C. Schumacher, A. Jacobo, A. McEnerney, A. Ramsey, G. Xu, D. Park, S. Kalomoiris, W. Yao, L. E. Jao, M. L. Allende, C. B. Lebrilla, F. A. Fierro, *Stem Cell Rep.* **2018**, *11*, 325.
- [12] T. Pizzute, J. Li, Y. Zhang, M. E. Davis, M. Pei, *Tissue Eng., Part A* **2016**, *22*, 1036.
- [13] X. Wu, Y. Jia, X. Sun, J. Wang, *Connect. Tissue Res.* **2022**, *63*, 256.
- [14] J. Xie, H. Bian, S. Qi, Y. Xu, J. Tang, T. Li, X. Liu, *Clin. Exp. Dermatol.* **2008**, *33*, 176.
- [15] M. Chang, C. Chen, Y. Chang, B. Zhong, Y. Wang, S. Yeung, H. Chang, J. Jeng, *J. Formosan Med. Assoc.* **2020**, *119*, 1666.
- [16] I. Carreras, C. B. Rich, M. P. Panchenko, J. A. Foster, *J. Cell. Biochem.* **2002**, *85*, 592.
- [17] G. Seghezzi, S. Patel, C. J. Ren, A. Gualandris, G. Pintucci, E. S. Robbins, R. L. Shapiro, A. C. Galloway, D. B. Rifkin, P. Mignatti, *J. Cell Biol.* **1998**, *141*, 1659.
- [18] Y. Hata, H. Kawanabe, Y. Hisanaga, K. Taniguchi, H. Ishikawa, *Cleft Palate Craniofacial J.* **2008**, *45*, 63.

- © 2023 The Authors. Advanced Healthcare Materials published by Wiley-VCH GmbH